UNIVERSITYᴼF BIRMINGHAM

Research at Birmingham

Photopolymerization of highly filled dimethacrylate-based composites using Type I or Type II photoinitiators and varying co-monomer ratios

Randolph , Luc D; Steinhaus, Johannes; Moginger, Bernhard; Gallez, Bernard; Stansbury, Jeffrey; Palin, William; Leloup, Gaetane; Leprince, Julian G

[Link to publication on Research at Birmingham portal](#)

Photopolymerization of highly filled dimethacrylate-based composites using Type I or Type II photoinitiators and varying co-monomer ratios

Luc D. Randolph[a, b, c, *]

luc.randolph@uclouvain.be

Johannes Steinhaus[d]

Bernhard Möginger[d]

Bernard Gallez[e]

Jeffrey Stansbury[f]

William M. Palin[g]

Gaëtane Leloup[a, b, c, h]

Julian G. Leprince[a, b, c, h]

[a]ADDB, Louvain Drug Research Institute, Université catholique de Louvain, ~~ELGIUM~~Brussels, Belgium

[b]Institute of Condensed Matter and Nanosciences, Bio- and Soft- Matter, Université catholique de Louvain, ~~ELGIUM~~Louvain-la-Neuve, Belgium

[c]CRIBIO (Center for Research and Engineering on Biomaterials), ~~ELGIUM~~Brussels, Belgium

[d]Bonn-Rhein-Sieg University of Applied Sciences, Department of Natural Sciences, von Liebig Str. 20, D-53359 Rheinbach, Germany

[e]REMA, Louvain Drug Research Institute, Université catholique de Louvain, ~~ELGIUM~~Brussels, Belgium

[f]Department of Chemical and Biological Engineering, University of Colorado, Boulder, CO 80309, USA

[g]Biomaterials Unit, University of Birmingham, College of Medical and Dental Sciences, School of Dentistry, St Chad's Queensway, Birmingham B4 6NN, UK

[h]School of Dentistry and Stomatology, Université catholique de Louvain, ~~ELGIUM~~Brussels, Belgium

*Corresponding author at: Université catholique de Louvain, Louvain Drug Research Institute, Avenue E. Mounier 73, B-1200 ~~ELGIUM*Corresponding author. Luc David Randolph,~~ Brussels, Belgium. Tel.: +32 483679738.

Abstract

Objectives

The use of a Type I photoinitiator (monoacylphosphine oxide, MAPO) was described as advantageous in a model formulation, as compared to the conventional Type II photoinitiator (Camphorquinone, CQ). The aim of the present work was to study the kinetics of polymerization of various composite mixtures (20 ~~40 60 — 40–60–~~80 mol%) of bisphenol A glycidyl dimethacrylate/triethylene glycol dimethacrylate (BisGMA/TegDMA) containing either CQ or MAPO, based on real-time measurements and on the characterization of various post-cure characteristics.

Methods

Polymerization kinetics were monitored by Fourier-transform near-infrared spectroscopy (FT-NIRS) and dielectric analysis (DEA). A range of postcure properties w~~ere~~as also investigated.

Results

FT-NIRS and DEA proved complementary to follow the fast kinetics observed with both systems. Autodecceleration occurred after ≈1 s irradiation for MAPO-composites and ≈ ~~5-5–~~10 s for CQ-composites. Conversion decreased with increasing initial viscosity for both photoinitiating systems. However despite shorter light exposure (3 s for MAPO vs 20 s for CQ-composites), MAPO-composites yielded higher conversions for all co-monomer mixtures, except at

20 mol% BisGMA, the less viscous material. MAPO systems were associated with increased amounts of trapped free radicals, improved flexural strength and modulus, and reduced free monomer release for all co-monomer ratios, except at 20 mol% BisGMA.

Significance

This work confirms the major influence of the initiation system both on the conversion and network cross-linking of highly-filled composites, and further highlights the advantages of using MAPO photoinitiating systems in highly-filled dimethacrylate-based composites provided that sufficient BisGMA content (>40 mol%) and adapted light spectrum are used.

Keywords: Photopolymerization; Dimethacrylate; Resin composite; Photoinitiator; Camphorquinone; MAPO; Kinetics; Dielectric analysis; Trapped radicals; Elution

1 Introduction

The polymerization kinetics of dimethacrylate-based resins have been extensively studied, particularly in relation to their application as dental restorative materials [1,2]. For this application, there is a specific demand for fast curing, highly filled resin-based materials, which are able to withstand the mechanical demand of masticatory load and degradative effects of the aqueous and frequently acidic environment. Glass and silica particles of micron and sub-micron dimensions, surface-modified with methacryl-functional silanes have been used as reinforcing fillers within dimethacrylate resin matrices. Free radical polymerization (FRP) is commonly used in these systems, initiated by light-sensitive molecules, which in most commercially available materials is a combination of camphorquinone (CQ) and a tertiary amine (Type II system). Specific curing mechanisms have been identified, most notably an autoacceleration and autodeceleration, associated with high polymerization rates, along with diffusion controlled termination and free radical entrapment [3–6]. Such fundamental work on polymerization kinetics was carried out with spectroscopic methods, mid or near-infrared spectroscopy being the most-used, but also with calorimetric and mechanical techniques such as differential scanning calorimetry [6–8] and dynamic mechanical analysis [9]. Amongst these studies, the effects of light irradiance, resin and photoinitiator chemistry have been studied.

Although previous work has provided useful information, many fundamental studies were conducted using unfilled resins, while dental restorative resin-based materials are reinforced with glass filler particulates to improve mechanical and physical material properties, typically up to 50–70 vol% (70–80 wt%) [10,11]. Few studies are available which report fundamental polymerization kinetics parameters in heavily filled resin composites. In these paste-like materials, light transport to deep layers is restricted due to, and amongst other factors, the presence of fillers and pigments, the absorption of photoinitiator molecules. Further, bulk viscosity is very high [12] and functional group conversion is lower than their resin counterparts [13].

Also, fundamental studies have focused primarily on detailing polymerization mechanisms in reactions using low light irradiance [5,14,15], (~50 mW/cm^2) in order to monitor polymerization under slower reaction rates. However, in highly filled resin composites, much higher light intensities are required to polymerize in depth [16] within acceptable curing times. Clinically relevant irradiances range from 500 to 3000 mW/cm^2, in general around 1000 mW/cm^2 used to light cure a ~2 mm thickness increment of conventional resin composite in ~20 s. Higher rates would be expected under such settings [13], affecting the polymer structure due to decreased chain length and increased amount of cross-links [17].

Furthermore, several photoinitiators (UV or visible, Type I or II) were used in the above-mentioned fundamental studies, without formal comparisons of their impact on polymerization kinetics. The Type II initiation system previously mentioned (CQ) absorbs in the visible range (400–500 nm; λ_{max} = 470 nm), while Type I molecules such as acylphosphine oxides absorb in the UV–vis region (λ_{max} ~380 nm) with a much higher absorption efficiency and radical yield [18,19]. Most interestingly for dental materials, their use in model dental resin-based composites led to shorter curing times (3–10 s [20], compared to 20 s with CQ). Several studies by our group focused on a model composite to compare the use of either a Type I (phenylbis(2,4,6-trimethylbenzoyl)phosphine oxide, MAPO) or a Type II (CQ) photoinitiating system [13,21–23]. The Type I-based composite presented faster kinetics under short irradiation times (1–3 s) and improved functional group conversion, reduced monomer elution and improved mechanical properties.

However the effect of such a potentially useful photoinitiation system within resins of varying viscosity is unknown. Further, determining the influence of kinetics on the formation of a cross-linked polymer network is also important to determine the effect of network structure on resulting mechanical properties.

Consequently, the aim here was to study the kinetics of polymerization of a series of BisGMA/TegDMA formulations, using either MAPO or CQ-based resins filled to 75 wt%. The study of polymerization kinetics will be the first objective of the present work and achieved by use of complementary methods adapted to appropriately follow fast polymerizations, i.e. near-IR spectrometry and dielectric analysis (DEA). These methods will be discussed with regard to their suitability to follow ultra-fast polymerizations. The second objective will be to further characterize the resulting polymer network of the cured materials by measuring elastic modulus and flexural strength by three-point bending, free monomer elution by reverse phase high pressure liquid chromatography (HPLC) and trapped free radicals by electron paramagnetic resonance (EPR).

2 Materials and methods

2.1 Materials

Bisphenol A glycerolate dimethacrylate (BisGMA, Sigma–Aldrich), triethylene glycol dimethacrylate (TegDMA, Sigma–Aldrich, 95%), initiator Camphorquinone (CQ, Sigma–Aldrich, 97%) with its co-initiator 2-(Dimethylamino) ethyl methacrylate (DMAEMA, Sigma–Aldrich, 98%) and initiator phenylbis(2,4,6-trimethylbenzoyl)phosphine oxide (MAPO, BASF) were used as received. Micro barium glass (G018-186/K6, d_{50} = 3 ± 1 µm, Schott AG, Landshut Germany) and nano silica (AEROSIL R7200, 12 nm, Evonik Industries, Germany), both methacryl-silane treated particles were also used as received.

2.2 Materials preparation

Four different BisGMA/TegDMA fractions were selected: 20/80, 40/60, 60/40 and 80/20 mol%. Two series were prepared by either using CQ/DMAEMA or MAPO in equimolar concentrations (0.20/0.80 wt% or 0.42 wt%, respectively), yielding a total of 8 different resin mixtures. In a final step, the micro and nano particles were introduced in amounts of 65 and 10 wt%, respectively. The resin composites were homogenized using a dual asymmetric centrifuge at 3500 rpm (Speed mixer, FlackTek, USA).

2.3 Methods – polymerization characteristics

Near-infrared spectra and ionic viscosities were recorded in real-time during irradiation and polymerization using Fourier-transform near-infrared spectroscopy (FT-NIRS) and dielectric analysis (DEA). In both methods, 2 mm-thick material layers were cured and analyzed. Such a thickness corresponds to the maximum thickness recommended in clinical settings, which is a major experimental difference compared to fundamental studies. In these, thin films were used to avoid issues with light transmission or variations in conversion, conditions suitable to extract intrinsic kinetic parameters. However the polymerization of dental resin composites occurs in non-ideal situations, in which high filler contents and thick layers (>1 mm) should be expected. Therefore, the present work intended to evaluate polymerization in a practical manner and in settings as close as possible to what would occur clinically.

FT-NIRS was performed in transmission mode (Nicolet6700, Thermo Scientific, Hemel Hemstead, UK) on disk shaped specimens contained in white Teflon moulds (12 × 2 mm). The system rested on a glass slide and was positioned so that the laser beam passing between two optic fibers was aligned with the center of the mold. The light tip was placed beneath and in contact with the glass slide, vertically aligned with the center of the mould. The degree of double-bond to single-bond conversion (DC) was followed through the variations of peak height located at 6164 cm^{-1}, attributed to vinyl CH_2 groups [24]. Absorbance data was collected for 120 s, at a sampling rate of 0.33 s^{-1}, with the first 10 s used prior to irradiation to establish initial absorbance ($A^{initial}$). DC was calculated according to Eq. (1), with $A(t)$ the absorbance at a given time

$$DC(t) = 1 - \frac{A(t)}{A^{initial}} \tag{1}$$

DC_{110s} was determined as the mean conversion value of the last 10 s of monitoring (Fig. 1). Conversion rates were determined as the first time derivative of DC. DEA was carried out using a previously described setup [25]. Briefly, a dielectric analyzer (DEA 231, Netzsch Gerätebau) was associated with a comb sensor (Mini-IDEX, 6 × 4 mm, electrode distance: 100 µm, Netzsch Gerätebau). As specified above, uncured material was placed in a 2 mm-thick layer atop the electrode, which was previously sprayed with technical grade silicone oil. The thickness of the composite layer was controlled by pressing a glass slide (1 mm thick) on top, with two glass slides placed on either sides of the electrode. A 1 kHz frequency was selected, corresponding to a sampling rate of 0.05 s^{-1}. Monitoring was performed for 120 s with the first 10 s used as signal baseline to determine initial viscosity (η_0^{ion}). Different parameters were determined as detailed in Fig. 1.
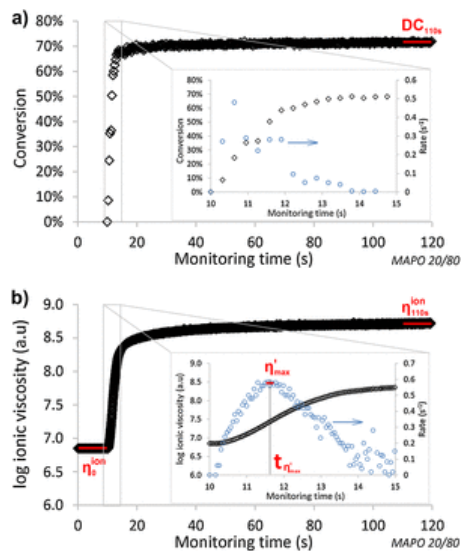
Fig. 1 Conversion and ionic viscosity as a function of monitoring time for MAPO 20/80 followed by FT-NIRS and DEA, respectively. The data was independently measured and show one sample only. The calculated variables are highlighted in red. Depending on the method and due to varying sampling rates, the determination of rates of signal change could not always be carried out (for example in a).

2.4 Irradiation conditions

Light irradiation was carried out with an AURA light engine (Lumencor Inc., USA), providing 2 discrete and independent spectral outputs, at 385–410 and 420–460 nm. The output adaptor was a 1 m quartz optic fiber (5 mm diameter). The incident irradiance was calibrated and set at 1000 mW/cm^2 for both spectral outputs, using a thermosensor (S310-C, Thorlabs, UK) connected to a PC via a USB converter (USB 100, Thorslabs). Further details are provided in the supporting information (S1). MAPO and CQ-composites were irradiated for 3 or 20 s respectively, based on previous works [21,23]. The corresponding radiant exposures, defined as the product of irradiance and irradiation time was hence 3 J/cm^2 and 20 J/cm^2.

2.5 Methods – post-cure material characterization

Using the previously detailed irradiation parameters, different samples were prepared for the analysis of post-cure properties, i.e. trapped free radical concentration, un-reacted monomers release and the flexural modulus and flexural strength. rectangular-shaped bars of 5 × 2 × 2 mm, disk-shaped specimens of 5 × 2 mm and bars of 25 × 2 × 2 mm, respectively were cured in white Teflon moulds for the different analyses. To the difference of samples used for kinetics evaluation, top and bottom surfaces of the bars were covered using polyester film during irradiation. The 25 × 2 × 2 bars were irradiated in five successive and non-overlapping cycles (light tip was 5 mm).

Trapped free radical concentration was determined by means of electron paramagnetic resonance (EPR) using a Miniscope MS200 EPR spectrometer (Magnettech, Germany), 1 h post irradiation. As previously described, the height of the fourth and fifth peak of typical nine-peak spectra were measured, corresponding to the concentration of trapped propagating and allylic radicals, respectively [26]. The following settings were used: 0.5 mW, microwave power; 336.7 mT, magnetic center field and 19.8 mT, field sweep; 0.1 mT, modulation amplitude. All measurements were carried out at ambient temperature (22 ± 2 °C) and in triplicates.

The release of un-reacted monomers was determined by means of reverse phase high pressure liquid chromatography (HPLC, Agilent 1100 series) equipped with a UV detector and a C18 column (140 × 4.6 mm, 3 μm particle diameter, BDS Hypersil, Thermo Scientific). Briefly, the 2 mm thick disks were each placed in 1 mL of 75/25 vol% ethanol/distilled water solution and left in the dark for one week at 37 °C ($n = 3$). Quantification was carried out for BisGMA and TegDMA, based on established calibration curves for the two monomers prior to testing (range 10–500 μg/mL). A gradient method was used, starting from a 60/40% H$_2$O/acetonitrile mixture and dropping to 0/100% over 19 min. Both reagents were of analytical grade.

Flexural modulus and strength were determined on bars busing a 3-point bending platform (LRX plus, Lloyd Instruments) with a 20 mm span between supports and a 0.75 mm/min crosshead speed ($n = 5$). The cured bars were stored for 1 week in 75/25 vol% ethanol/distilled water, at 37 °C prior to reflect the conditions for the release study. Mechanical properties were determined using standard formulas of beam theory.

2.6 Statistical analysis

Regressions and their determination coefficients (R^2) were determined using Excel (Microsoft) and Spearman correlations coefficients were established using JMP 11 (SAS Institute Inc.). When p-values were higher than 0.01, values were specified.

Comparison of the photoinitiator effect at a given co-monomer ratio was carried out using one-way ANOVA and student's t-test at a 0.05 significance level.

3 Results and discussion

3.1 Methodological considerations

FT-NIR spectroscopy and DEA were used as complementary methods in the measurement of ultra-fast polymerization kinetics of highly filled resin-composite systems cured in thick layers. Whilst FT-NIRS measures the change in absorption related to the concentration of vinyl double bonds, DEA provides a measurement of the variation in amplitude and phase shift in an electric signal, both indicating variations in dielectric properties, namely permittivity ε' and loss factor, ε''. Ionic viscosity (η^{ion}) is approximated as

$$\frac{1}{\sigma} = \frac{1}{\varepsilon'' \varepsilon_0 \omega}$$

(2)

considering the conductivity (σ) to be frequency (ω) independent. η^{ion} directly reflects mechanical viscosity ($1/\sigma = 1/(q \times \mu \times n)$ where q is the charge of ions, μ is the mobility of ions and n is their concentration) as ion mobility is directly affected by diffusion, which is controlled by mechanical viscosity. However with FT-NIR spectroscopy the determination of conversion is more straightforward, as long as $A^{initial}$ is reliably collected prior to polymerization. It is therefore quite commonly used to study kinetics in resin composites. According to the literature, DEA applied to the monitoring of cure in thermosets may be calculated using Eq. (3):

$$DC(t) = \frac{\log(\eta_0^{ion}) - \log(\eta_t^{ion})}{\log(\eta_0^{ion}) - \log(\eta_\infty^{ion})}$$

(3)

where the subscripts indicate the moment at which η^{ion} is determined. This was proposed in the case of epoxy resins [27], a system which may reach complete conversion of its functional groups, unlike the dimethacrylate-based resin-composite used in the present study. In the case of this system utilizing free radical polymerization at relatively low temperature, conversion is inherently limited [13,28] and in the absence of reference, DEA can only provide qualitative results. Hence, in the present work, final ionic viscosity (η_{110s}^{ion}, Fig. 1) was reported but not correlated to relative conversion values.

FT-NIRS may lack resolution in the first few seconds to accurately determine Rp, due to a limited sampling time. Comparatively, DEA is much more reliable at early stages of the reaction, before viscosity increases by several orders of magnitude [25]. At the same time, DEA allows for the collection of many more data points per unit time compared with FT-NIRS. However, when polymerization proceeds and monomer mobility becomes so low that differences between ionic conductivity and thermal noise are negligible, accuracy decreases and DEA becomes less efficient. On the contrary, FT-NIRS is then much more stable as the refractive index of the resin gets in general closer to that of the fillers [29], effectively improving light transmission throughout the curing resin composite and leading to an improved signal-to-noise ratio. More importantly, as the micro glass particles used in this study have a refractive index of 1.55 (manufacturer's data) and noting that un-cured resins containing increasingly higher fractions of BisGMA display higher indices, from 1.474 to 1.534 (for BisGMA contents of 6–76 mol% [30]), the initial translucency of the resin composites would vary. In addition, as mentioned above, the translucency during curing changes, for example with a 76/24 mol% resin having its index change from 1.534 to 1.560 [30]. These values bracket the filler index and optimum translucency would be reached during curing. It would follow that the overall energy provided to the material actually varies during the polymerization, affecting kinetics most significantly when the translucency is highest at the point of higher rate of polymerization.

Other characterization methods could be considered but they may present some limitations. Briefly, alternatives such as photorheology [9] would prove difficult due to the initial high viscosity of resin composite. Differential scanning calorimetry (DSC) would pose other issues, mainly regarding thermal effects from the irradiation, which would be difficult to de-correlate from polymerization itself. DSC sample size and ratio which has been shown to influence light transmission [31] would also be clinically irrelevant. Sampling time may also be limited.

FT-NIRS and DEA suggest suitable complementary methods to follow ultra-fast polymerization kinetics. Specifically for MAPO 20/80, while Rp could not be reliably determined (Figs. 1, 2a and 2b), a rate of change in η^{ion} could be followed. From the average curves shown in Fig. 2a and b, a double maxima was observed, a pattern reported and discussed elsewhere [6,32]. Such variations in rate were associated with changes in reactivity of pendant groups. In the present work, we suggest that this was an artifact and draw the attention of the reader to Fig. 1a, where the rate for one measurement is plotted. Given the dispersion and insufficient sampling time, when average curves of three measurements are produced (such as in 2a), the noise accumulates and yields fictitious variations. In the later stages of polymerization however, when the polymer matrix became highly cross-linked, FT-NIRS gained in accuracy as rates dropped while noise tended to alter the signal collected with DEA (as noted above). This may be observed in Fig. 2 where the dispersion of data points in c) and d) is considerable, in particular in BisGMA-rich materials, and almost absent from (a) and (b). As a consequence, maximum rates of change in η^{ion} could not always be determined, such as for CQ 60/40 and CQ 80/20 and instead FT-NIRS appeared more suited. The two techniques also provided complementarity data with regards to polymerization characteristics: the time to reach $\dot{\eta}_{max}^{ion}$ ($t_{\dot{\eta}_{max}^{ion}}$, where $\dot{\eta}^{ion} = d\eta^{ion}/dt$) could be determined with DEA and the values fitted to FT-NIRS data to observe conversion at that point. To some extent, this approach circumvented the limitations of FT-NIRS in determining Rp^{max} and $t_{Rp^{max}}$. However η^{ion} evolved slightly more slowly than conversion, most likely due to the difference in setup; with DEA, the bottom 0.1 mm was analyzed [43], compared to the bulk of the 2 mm-layer with FT-NIRS. Nevertheless, $t_{\dot{\eta}_{max}^{ion}}$ accurately located the end of autoacceleration as a change in the rate of η^{ion} and certainly corresponded to the onset of diffusion-controlled termination [15].

Fig. 2 Rates of change for the polymerization of MAPO and CQ-composites (note the different time scale). Analysis was carried out with FT-NIRS (a and b) or DEA (c and d). The curves show an average of three repeat measurements. The resin composition is indicated by BisGMA/TegDMA in mol%.

The light shut-off is located by dotted lines.

3.2 Kinetics of polymerization

MAPO-composites exhibited much faster kinetics of polymerization compared to those based on CQ (Figs. 2 and 3) using both FT-NIRS and DEA. MAPO-composites exhibited Rp^{max} values that were higher (up to 10 times) than their CQ-equivalents. Confirming the visual trend observed in Fig. 2c and 2d, $t_{\dot{\eta}^{ion}_{max}}$ values were 5 times lower in MAPO-composites (Table 1), further highlighting the much faster reaction rates compared with CQ-composites. When extrapolating conversion at $t_{\dot{\eta}^{ion}_{max}}$, higher values (in the range 30—40%) were reached in MAPO-composites compared with CQ-composites (about 20%). The time necessary to reach 95% of DC_{110s}, $t_{DC_{95\%}}$, was from 4 to 6 times greater in CQ-composites (Table 1). These results indicated major differences in polymerization behaviors and will be discussed further.

Fig. 3 Evolution of conversion and ionic viscosity with time in MAPO and CQ-composites (note the different time scales), followed with FT-NIRS (a and b) or DEA (c and d). The curves show an average of three repeat measurements. The resin composition is indicated by BisGMA/TegDMA in mol%.

Curing parameters were 1000 mW/cm^2 for 3 and 20 s, respectively. The light shut-off is located by dotted lines.

Table 1 Characteristics determined using DEA and FT-NIRS for the photo-polymerization of MAPO and CQ-based resin composites. $t_{\dot{\eta}^{ion}_{110s}}$ was calculated on log-treated curve seconds.

Photoinitiator	BisGMA/TegDMA ratio (mol %)	t_{Rp}^{max} (s)	$t_{DC_{95\%}}$ (s)	$\Delta DC_{off\to100s}$ (%)	$\dfrac{\Delta DC_{off\to100s}}{DC_{110s}}$ (%)
MAPO	20/80	1.6 (0.1)	5.9 (1.5)	8 (3)	11
	40/60	1.0 (0.1)	6.3 (0.3)	6.6 (0.1)	9
	60/40	1.0 (0.1)	8.0 (0.7)	6.8 (0.4)	11
	80/20	1.5 (0.2)	12.4 (0.8)	7.4 (0.8)	14
CQ	20/80	9.1 (0.5)	21.5 (1.6)	4.7 (0.2)	7
	40/60	5.2 (0.2)	36.9 (1.7)	6.4 (0.3)	11
	60/40	×	50.1 (5.1)	6.5 (0.3)	14
	80/20	×	63.2 (3.0)	6.8 (0.7)	18

x symbol indicates that no value could be determined due to high noise. Standard deviations in parentheses. $\Delta DC_{off\to100s}$ indicate the difference in conversion between the light shut-off and after 110 s.

In the fundamental studies published previously, the light source was usually kept on throughout the monitoring sequence. However, in such cases, the radiant exposure (J/cm^2) may far exceed that required for optimal polymerization and in certain cases be much higher than in clinical settings. Moreover, the radiant exposure required to reach this optimum has been shown to vary substantially from one photoinitiating system to another. Values of 3 J/cm^2 were reported for MAPO systems [21,23], whereas values around 20 J/cm^2 are frequently referenced for CQ systems [13,54]. In the present work, these reported optimal radiant exposures of 3 J/cm^2 and 20 J/cm^2 were used for MAPO and CQ-composites, respectively. It is worth mentioning that these values are obtained using light emitted at the narrow wavelength ranges described earlier. Also, the similar irradiance chosen for both ranges (1000 mW/cm^2) is relevant to the blue light component emitted by commercially available light curing units, but is much higher than the violet light component currently distributed (around 200 mW/cm^2 [65]). The short curing times and high irradiances used in the present work for MAPO systems resulted in higher polymerization rates than those reported in previous studies (0.002–0.004 or 0.0022–0.0253 s^{-1} for Rp^{max} [6,7]), confirming the influence of high irradiance [76]. Conversion continued to increase after the light was stopped, which is already well understood [3,87] and in accordance with our previous studies [13,21,22], most significantly for CQ-composites (Table 1, $\Delta DC_{off\to110s}/DC_{110s}$ ratio), highlighting a difference in the extent of dark-cure. The differences between $t_{DC_{95\%}}$ and irradiation times also indicated polymerization continuing well after the light was stopped, and provides further evidence of the post-cure reaction [98]. Changes in ionic viscosity following 20 s light cure (Fig. 2d) also further demonstrated this dark-cure phenomenon.

Additional polymerization characteristics could be specifically extracted from the DEA curves (Fig. 2c and 2d). First, a decrease in ionic viscosity was observed in the first few seconds following the start of irradiation, before viscosity increased exponentially. The decrease was most markedly observed in CQ-based composites and associated with the temperature increase due to the irradiation. The slower the polymerization, the clearer the effect of the light could be observed. Second, additional signs of the influence of irradiation could be seen when the light irradiation stopped in CQ-composites, resulting in the observed inflection at ~20 s (Fig. 3d) and a sudden increase in rate of change of ionic viscosity. A volumetric contraction is in fact known to take place at that point as the temperature inside the resin sample was brought well above room temperature, while most of the polymerization reaction has occurred and is no longer a main contributor to heating at that point [39]. Thermodynamics then dictates a sudden decrease of volume ($dV/V = \alpha dT$, here with $dT < 0$ and with α the volumetric thermal expansion coefficient), in turn translating at the molecular level into reduced mobility and hence a step in ionic viscosity.

With both MAPO and CQ-composites, the highest DC_{110s} was observed for the formulations containing 20 mol% BisGMA, at 72% and 69.7%, respectively (Fig. 4a). The monitoring of ionic viscosity by DEA indicated inverse trends, with the 20/80 composites displaying the lowest values. However the final ionic viscosity (η_{110s}^{ion}) of CQ 20/80 was higher than its MAPO equivalent, contrary to the rest of co-monomer mixtures (Fig. 4b). Several factors have been described that would influence η_{110s}^{ion} . According to Anseth et al. [15], high rates of polymerization would be associated with excess free volume, which was observed as lower permittivity, i.e. higher ionic viscosity in the present investigation. This phenomenon would occur in parallel with an increase in cross-linking and amount of trapped radicals, both of which decrease ionic viscosity. Since there was no way to identify the prevalence of one factor over the other, no conclusions could be provided. However two trends could still clearly be identified: DC_{110s} and η_{110s}^{ion} values were observed to respectively decrease and increase with increasing BisGMA content, with excellent linear correlation, clearly dependent on the photoinitiator type (Fig. 4). Consequently, it appears that the fraction of the viscous monomer pre-determined the extent of conversion.
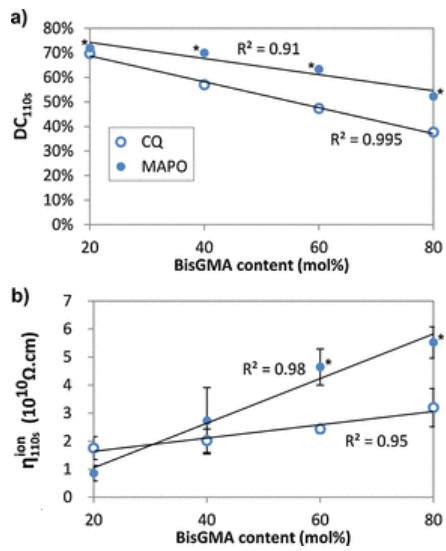
...

Fig. 4 ~~a) conversion and~~ (a) Conversion and (b) ionic viscosity values after 110 s of monitoring for MAPO and CQ-composites as a function of BisGMA content. ~~RF~~R^2 are the coefficients of determination for the linear regressions. Error bars correspond to standard deviations (symbols may hide the error bars). * ~~s~~Symbols indicate a significant difference (~~pp~~p < 0.05) between the MAPO and CQ series, for one resin composition.

It is widely acknowledged that amongst other characteristics, the initial viscosity and composition pre-determine the extent of polymerization, through mobility restriction, with the onset of autoacceleration and the onset of diffusion-controlled termination being moved to earlier stages of conversion [6,7,3~~7~~6]. In previous studies, the optimum conversion, that is the highest conversion that could be obtained in a range of formulations, was determined to coincide with high rates. This in turn was associated with a specific initial viscosity. In the present work, the maximum conversion with either photoinitiating system was observed in mixtures with low BisGMA content (20 mol%; Fig. 3), while the noted studies usually locate this optimum around 50 mol%. This shift is most likely due to the local viscosity increase in the resin imparted by the fillers. In addition, the silanated fillers contribute to a significant fraction of reactive groups and conversion of the surface bound methacrylates would be more extensive with lower viscosity resins. The initial ionic viscosity (η_0^{ion}) showed an exponential increase with BisGMA content (Fig. 5a). Hence, in addition to the previously described linear correlation between DC_{110s}, η_{110s}^{ion} and BisGMA/TegDMA ratio, variations in η_0^{ion} confirmed that molecular mobility already varied greatly in the un-cured materials. Besides co-monomer ratio, the photoinitiator system clearly affects the relationship between monomer composition and polymerization efficiency. Based on the much greater absorption efficiency and quantum yield of MAPO compared with CQ [41,42~~0,41~~], it was originally hypothesized that MAPO would yield higher conversions than CQ regardless of the resin composition. As such, while the initial viscosity was previously found to play a major role, the extent of polymerization could instead be dominated by the initiator efficiency. This hypothesis was also supported by the higher conversion and radical concentration observed with MAPO in a model resin composite (70/30 wt% (81/19 mol%) BisGMA/TegDMA) [23]. However, as presented by Figs. 4 and 5, η_0^{ion} , DC_{110s} and η_{110s}^{ion} variations with co-monomer ratio contradicted that hypothesis, since higher conversions in MAPO compared with the CQ-based composites were only observed for mixtures containing 40 mol% BisGMA or more. In fact the composites containing 20 mol% BisGMA were an exception, since similar conversion values were obtained with both photoinitiating systems and DC_{110s} were also the highest of the tested conditions (~70%). This observation could be explained by high molecular mobility and a high double bond density, conditions required to encourage delayed reaction diffusion-controlled termination. In such case, a high conversion in the lesser efficient Type II system was observed, comparable to the Type I. Lovell et al. determined in unfilled resins that a minimum of 25 wt% BisGMA (37 mol%) would be required to reach the optimum conversion in CQ-based co-monomer mixtures [5]. Again, the difference observed with the data presented here (20 mol% vs 40 mol% or more) should be associated with the fillers. A general and clear inverse correlation between η_0 and DC_{110s} was observed in both photoinitiating systems (Fig. 5b). Likewise, η_{110s}^{ion} values relative to initial viscosities also decreased with initial viscosity and most precisely according to a power law for CQ-composites (Fig. 5c). Definite conclusions could be drawn from these observations. Firstly, increased initial viscosity led to a significantly decreased conversion due to reduced molecular mobility. Secondly, and reflecting the difference in ranges for conversion in MAPO and CQ-composites, the latter series appeared more influenced by η_0^{ion} , with DC_{110s} decreasing to a greater extent (from 69.7 to 37.7% compared to 72.0 ~~to~~ 52.3% for MAPO-composites). Also, significant differences in η_{110s}^{ion} with CQ-composites were noted above 40 mol% BisGMA (Fig. 4) while there was also a lack of variation between 20/80 and 40/60 MAPO in η_{110s}^{ion} expressed relatively to η_0^{ion} . Given the more complicated initiation step of camphorquinone (excitation to triplet state and hydrogen abstraction from the tertiary amine [4]) it can be assumed that at a given concentration of initiator and co-initiator, the more viscous mediums would hinder diffusion and the potential for activation, even more as conversion progressed. Due to its simpler initiation step, the Type I system would be less sensitive. Hence, while fundamental studies have established that final conversion increases with decreasing viscosity, with both Type I [37,38~~6,37~~] or Type II systems [3~~8~~7], the present results suggested that Type I-based composites were less affected.
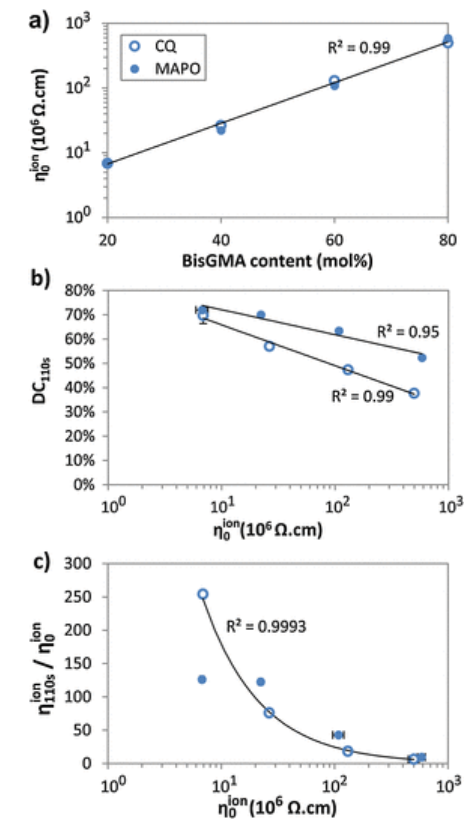
Fig. 5 (a) initial ionic viscosity as a function of BisGMA content, ~~b) conversion versu~~(b) conversion vs initial viscosity and (c) ionic viscosity at 110 s divided by initial ionic viscosity as a function of initial viscosity for the CQ and MAPO composites (empty and filled circles, respectively). ~~R~~R^2 indicate the regression coefficients for exponential (in a), logarithmic (in b) and power law (in c) regressions. Deviations represent the standard deviations of three measurements (and may be hidden by symbols). * ~~s~~Symbols indicate a significant difference (~~p~~p < 0.05) between the MAPO and CQ series, for one resin composition.

Assuming a bimolecular termination, the change in the concentration of radicals can be described such as [~~43];(4)d~~R2]:

$$\frac{d[R^\bullet]}{dt} = R_i - 2k_t[R^\bullet]^2 \qquad (4)$$

where R_i is the initiation rate and is also equal to $2\phi I_a$ (2 radicals/initiator molecule, ϕ is the quantum yield for initiation and ~~I~~I_a the absorbed light intensity), ~~R~~$[R^\bullet]$ is the concentration of radicals, and k_t is the termination constant. In the absence of initiation, the propagation rate becomes related to the concentration of radicals according to [~~4~~32]:

$$R_p = k_p[M][R^\bullet] \qquad (5)$$

where k_p is the propagation constant and ~~M~~$[M]$ is the concentration of double bonds. However, both monomolecular and bimolecular termination take place and the rate dependence on initiation then becomes much more complex [~~4~~32]. Due to the possibility of a radical to react with a pendant group on its own kinetic chain (primary cycle) or on a different chain (secondary cycle), and the higher reactivity of such pendant groups at low conversion, cyclization may occur [~~4~~43]. Dickens et al. have suggested initial viscosity "influenced the reaction rates up to the point when autoacceleration stopped" (BisGMA/TegDMA mixtures, CQ/ethyl 4-(dimethylamino)benzoate as photoinitiating system) [6]. In the present investigation, an obvious difference in rate behavior as conversion or ionic viscosity increased could be observed between MAPO and CQ-composites (Fig. 6). Rates of change were always higher in MAPO than in CQ-composites (Fig. 7), confirming the higher efficiency of the MAPO system. When investigating correlations, η_0^{ion} was found to be positively correlated to the maximum rate of change in ionic viscosity (η_{max}^{ion}) (0.47 (~~p~~p = 0.0670) and 0.95 for CQ and MAPO-composites, respectively). Further, total ionic viscosity changes could be considered relatively to η_0^{ion} to analyze the extent of mobility variations. It was found that with increasing maximum rates, the $\eta_{110s}^{ion}/\eta_0^{ion}$ ratio decreased, in both series (Fig. 7). This is in line with previously reported observations [6] which noted that increased initial viscosity yields an onset of autodeceleration at lower conversion (Fig. 6) and presently would be observed as a decreased $\eta_{110s}^{ion}/\eta_0^{ion}$ ratio (lower final conversion). Interestingly, Lovell et al. observed a positive trend between polymerization rates and final conversion (75/25 BisGMA/TegDMA resin, Type I

photoinitiating system) [3,8,7]. In other words, for a specific initial viscosity, higher polymerization rates allow the polymerization reaction to proceed further before deceleration occurs. The present results however show that this is not valid when comparing systems of different viscosities, and hence reactivity, for which maximum rates and final conversion are not correlated [3,7,6].
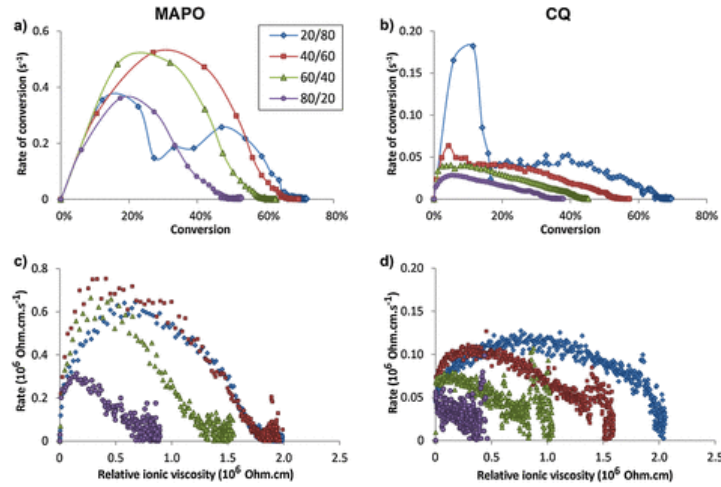

Fig. 6 Rates of change as a function of conversion or ionic viscosity for the polymerization of MAPO and CQ-composites (note the different vertical scales). Analysis was carried out with FT-NIRS (a and b) or DEA (c and d). The curves show an average of three repeat measurements. The resin composition is indicated by BisGMA/TegDMA in mol%.
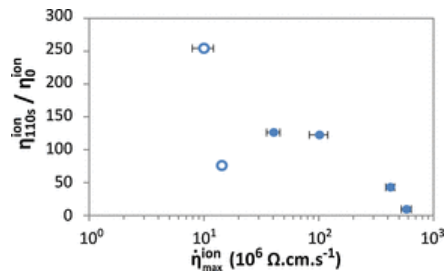

Fig. 7 ionic viscosity at 110 s divided by initial ionic viscosity as a function of maximum rate of change in ionic viscosity ($\dot{\eta}_{max}^{ion}$), for CQ and MAPO-composites (empty and filled circles respectively). Error bars indicate standard deviations.

3.3 Post-cure material properties

Radical trapping was noted to occur at every stage of polymerization, first due to cyclization and then due to a general loss of mobility following vitrification. Depending on the initiation efficiency, the amount of radicals generated would also vary. The quantification of trapped radicals following polymerization hence provided further information on the extent of the reaction in the composites and was measured using EPR (Fig. 8). As expected, based on previous work [23], the quantity of allylic and propagating radicals was greater in MAPO-composites compared with CQ-composites, except at 20 mol% BisGMA where they were similar. For CQ-composites, a positive correlation between DC_{110s} and radical concentration was observed (0.91 and 0.85 for propagating and allylic radicals respectively) while a negative one was observed between η_{110s}^{ion} and radical concentration (−0.89 and −0.83). On the contrary in MAPO-composites, DC_{110s} and η_{110s}^{ion} were negatively and positively correlated to radical concentration, respectively (−0.79/−0.75 and 0.85/0.80 for allylic/propagating radicals). The opposite trends between initiating systems originated from the different polymerization kinetics, more specifically from the higher polymerization rates in MAPO-composites. As noted above, increased radical trapping would occur the faster the polymerizing network reached autodecceleration and also leading to lower final conversions. However and as already noted, the Type I system remained more efficient over the range of formulations. Based on all the different considerations discussed, major structural differences in terms of polymer network could be expected between MAPO and CQ-composites as conversion varied but even more important, it progressed coupled with BisGMA content.
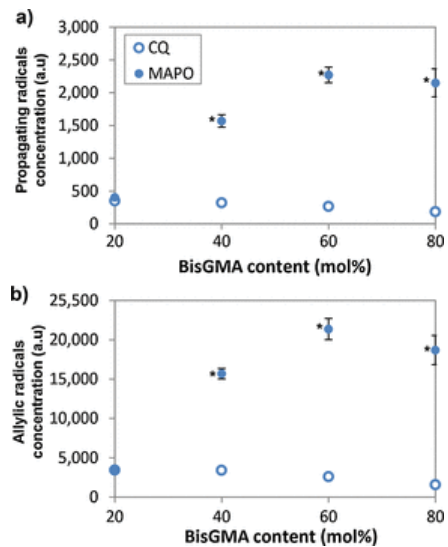
a)

b)

Fig. 8 Trapped radicals concentration in CQ and MAPO-composites (empty and filled circles, respectively). Radical concentration determined 1 h following irradiation. * ~~s~~Symbols indicate a significant difference (~~p~~p < 0.05) between the MAPO and CQ series, for one resin composition.

Polymer networks within resin composites may differ in chain length and cross-link density, or fraction of pendant methacrylate groups and unreacted monomers, which do not contribute to cross-linking. Measurement of unreacted monomer release provided useful information on the differences in polymer network within the cured materials. The use of an ethanol-based solution provided good solubility for both TegDMA and BisGMA which are moderately hydrophobic (Nernst partition coefficients were measured at 2.2 and 1.3, respectively in octanol/PBS) [4~~5~~4]. The solution included water as it has been previously shown that a TegDMA-resin would absorb higher amounts of liquids in a mixed solution than in either pure ethanol or water [4~~6~~5]. Diffusion of liquids was also higher, which in turn would translate into a more efficient removal of unreacted monomers. Aqueous ethanol solutions are hence often encountered as release mediums in the literature [4~~7~~6]. In the present work, monomer release was strongly and inversely correlated with the degree of conversion, a result in line with previous studies [14,23]. The non-linear and inverse correlation was however only strongly observed for CQ-composites (~~-0.93 and -~~-0.93 and -0.92 for BisGMA and TegDMA, respectively) and not for MAPO-composites. As one may observe in Fig. 9a, MAPO 20/80 released the highest amount of monomers, while also displaying the highest conversion. The difference was tentatively associated with the high density of double bonds in the resin composite containing 20 mol% BisGMA. In the case of polymerization with a type I photoinitiator, the ultra-fast kinetics and high efficiency of initiation would lead to a high conversion but also to a highly cross-linked network and a comparatively reduced monomer addition. By increasing BisGMA content to 40 mol%, the initial density of double bond would decrease by 10%. As propagation proceeds diffusion-controlled, the lower density would evidently encourage monomer addition and hence yield a significantly lower monomer release. Beside this discrepancy, MAPO-composites overall displayed lower amounts of monomer released compared to CQ-composites, even when associated with lower conversions. This further supported the hypothesis made on the impact of kinetics and efficiency of initiation. Further, with both initiation systems, greater amounts of BisGMA were released compared to TegDMA, in all co-monomers formulations. As stated previously, during polymerization, the contribution of free monomer addition or cross-linking may vary. A greater contribution from monomer addition would translate into a shift to higher gel fractions, for a given conversion. Inversely, cross-linking does not involve the binding of a free monomer to the developing network, and, for the same conversion, a shift to lower gel fraction would be observed. In addition, in a co-monomer system, the different molecules are not depleted evenly during polymerization. In the present work, TegDMA was released in smaller quantities relative to its initial proportion as compared with BisGMA (Fig. 9b and c). This smaller release of TegDMA was due to its preferential addition compared to the bulkier and more rigid BisGMA [14]. In addition, given the non-linear relationship between monomer release and conversion, the overall predominance of monomer addition over cross-linking was evident.
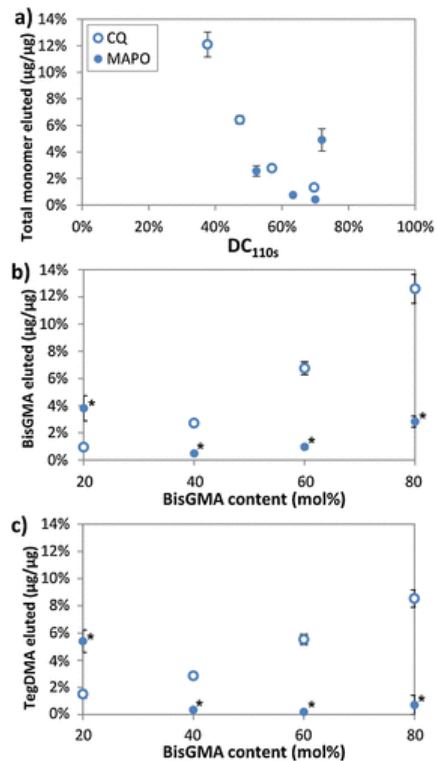
Fig. 9 Total monomer release (sum of BisGMA and TegDMA eluted, in relative amounts) as a function of DC_{110s}. (a). BisGMA (b) and TegDMA (c) release from cured specimens after 1 week storage in 75/25 $EtOH/H_2O$ as a function of BisGMA content used for the initial resin formulation. Error bars indicate standard deviations. * symbols indicate a significant difference (~~p~~ $p < 0.05$) between the MAPO and CQ series, for one resin composition.

The highest flexural modulus and strength were observed for MAPO 40/60, MAPO 60/40 and CQ 20/80 (Fig. 10). Except for MAPO 20/80, all MAPO-composites displayed equal or higher flexural modulus and strength compared to CQ-composites. Both properties were strongly and linearly correlated to one another, both for MAPO and CQ-composites (0.97 and 0.99 respectively). Considering other characteristics, for example monomer elution, a strong and inverse correlation to flexural modulus (~~-0.93/-0.74 for MAPO and -0.87/-~~ −0.93/−0.74 for MAPO and −0.87/−0.90 for CQ-composites, BisGMA/TegDMA respectively) and flexural strength (~~-0.93/-0.81 for MAPO and -0.88/-~~ −0.93/−0.81 for MAPO and −0.88/−0.92 for CQ-composites, BisGMA/TegDMA respectively) was observed. Conversion in CQ-composites was positively correlated to both flexural modulus and strength (0.97 in both cases).
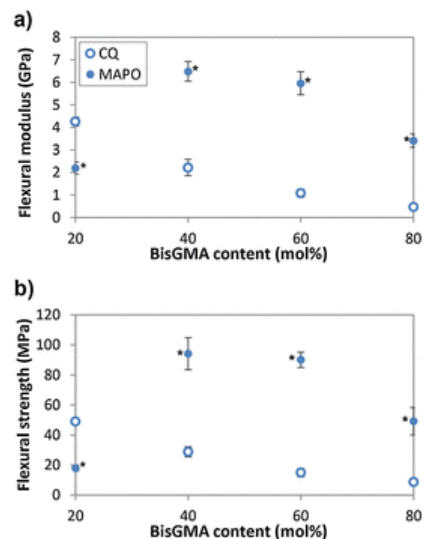
a)

b)

Fig. 10 (a) Flexural modulus and (b) flexural strength for MAPO and CQ-composites following a one week incubation in 75/25 vol% ethanol/water solution (filled and empty circles, respectively). * Symbols indicate a significant difference ($p < 0.05$) between the MAPO and CQ series, for one resin composition.

The flexural modulus of a composite material depends on filler load, the interface between the resin and fillers (consisting of methacryl-silanes) and the extent of resin and silane polymerization. With resin composites filled with a bimodal filling, the fumed silica of a mean size of 12 nm can be viewed as directly reinforcing the resin itself, assuming that they are well dispersed. Micro glass particles provide stiffness ($E = 77$ GPa, manufacturer information) but also increase strength, for example through crack deflection. In the resin composites prepared here, a constant filler mass percentage was used and the only variable effecting mechanical properties was the resin itself, possibly along with the quality of the interface. The ethanol-based storage medium also further any exacerbated network differences by favoring solvent sorption, elution and degradation mechanisms, compared to simply water [45]. From the previous discussion, it could be expected that due to overall lower conversion and higher monomer elution, both indicative of weaker polymer matrices, CQ-composites would present relatively low mechanical properties compared to MAPO-composites for which comparatively higher conversion, radical concentration and lower monomer elution were noted. The results showed that for CQ-composites, with increasing BisGMA content, mechanical properties decreased, as expected from the decreasing conversion. However for MAPO-composites, an optimum was noted at 40 and 60 mol% BisGMA, although conversion was highest at 20 mol%. To explain this trend, it may be recalled that conversion decreased by only 2% between MAPO 20/80 and 40/60. At the same time, the 20 mol% increase of BisGMA would necessarily equivocate to a polymer matrix comprising a higher fraction of the stiffer molecule. In addition, the high trapped radical concentration, which reached a plateau at 60 mol% suggested highly cross-linked networks. The optimum in mechanical properties hence corresponded to the co-monomer composition for which a high conversion, extensively cross-linking and BisGMA-rich network was generated. To explain the lower values at 20 or 80 mol% BisGMA, it may be reminded that overall ultra-fast kinetics were observed with MAPO-composites. At 20 mol%, this would depress the reactivity of methacrylate groups bound to filler particles, comparatively to the monomers. The high amount of monomers eluted despite the high conversion at this composition was associated to extensive cross-linking but may also be related to a reduced conversion of the bound methacrylates. This would yield a soft and fragile resin composite (low modulus and strength, respectively). Increasing the BisGMA content reduced monomer mobility, as shown by the increasing η_0^{ion} , decreased the double bond density and the difference in reactivity between bound and free methacrlayte groups was likely reduced. The more converted the particle/resin interface, the more coherent it would be. As defect propagation occurs at the interface [47], for a given surrounding polymer network, a higher strength would result from an improved conversion of the bound methacrylates. Further, the higher mechanical properties of CQ 20/80 compared to MAPO 20/80 could then be attributed to the slower kinetics of the Type II photoinitiator: the bound methacrylates would benefit from longer reaction times, favorable to chain relaxation.

4 Conclusions

- With increasing BisGMA fraction, the ionic viscosity of uncured pastes increased, indicative of decreasing molecular mobility

- Monitoring the polymerization by DEA and FT-NIRS proved suitable to follow ultra-fast reactions, with DEA being more accurate in the first instants of the polymerization, while FT-NIRS accurately informed on the conversion at latter stages

- The experimental CQ-composites exhibited lower polymerization rates than MAPO-composites, which also displayed higher conversions, when photopolymerized under clinically-relevant conditions (1000 mW/cm^2, for 20 and 3 s, respectively)

- For BisGMA fractions of 40 mol% or more, increased trapped radical concentration, reduced monomer elution and higher mechanical properties were observed in MAPO-composites compared to CQ-composites, confirming the higher efficiency of MAPO

- Finally, a lack of linearity between the quantity of un-reacted monomers and conversion highlighted the extensive cross-linking of the dimethacrylate-based resin composites. This was possibly related to more complete polymerization reactions, in particular of the filler-bound methacrylate

groups. The resin viscosity and initial double bond density must be balanced so that the reactivity of free monomers does not depress that of the bound molecules

Acknowledgement

Appendix A. Supplementary data

Supplementary data associated with this article can be found, in the online version, at http://dx.doi.org/10.1016/j.dental.2015.11.032.

References

[1]

J.G. Leprince, W.M. Palin, M.A. Hadis, J. Devaux and G. Leloup, Progress in dimethacrylate-based dental composite technology and curing efficiency, *Dent Mater* **29**, 2013, 139–156.

[2]

N.B. Cramer, J.W. Stansbury and C.N. Bowman, Recent advances and developments in composite dental restorative materials, *J Dent Res* **90**, 2011, 402–416.

[3]

K.S. Anseth, C.M. Wang and C.N. Bowman, Kinetic evidence of reaction diffusion during the polymerization of multi(meth)acrylate monomers, *Macromolecules* **27**, 1994, 650–655.

[4]

W.D. Cook, Photopolymerization kinetics of dimethacrylates using the camphorquinone/amine initiator system, *Polymer* **33**, 1992, 600–609.

[5]

L.G. Lovell, J.W. Stansbury, D.C. Syrpes and C.N. Bowman, Effects of ~~Composition and Reactivity on the Reaction Kinetics of Dimethacrylate/Dimethacrylate C~~composition and reactivity on the reaction kinetics of dimethacrylate/dimethacrylate copolymerizations, *Macromolecules* **32**, 1999, 3913–3921.

[6]

S.H. Dickens, J.W. Stansbury, K.M. Choi and C.J.E. Floyd, Photopolymerization ~~Kinetics of Methacrylate Dental R~~kinetics of methacrylate dental resins, *Macromolecules* **36**, 2003, 6043–6053.

[7]

L. Feng and B.I. Suh, Exposure ~~Reciprocity Law in P~~reciprocity law in photopolymerization of ~~Multi-Functional Acrylates and M~~multi-functional acrylates and methacrylates, *Macromol~~ecular Chemistry and Physics~~ Chem Phys* **208**, 2007, 295–306.

[8]

M. Rosentritt, A.C. Shortall and W.M. Palin, Dynamic monitoring of curing photoactive resins: a methods comparison, *Dent Mater* **26**, 2010, 565–570.

[9]

J.W. Stansbury, Dimethacrylate network formation and polymer property evolution as determined by the selection of monomers and curing conditions, *Dent~~al Materials~~ Mater* **28**, 2012, 13–22.

[10]

J. Leprince, W.M. Palin, T. Mullier, J. Devaux, J. Vreven and G. Leloup, Investigating filler morphology and mechanical properties of new low-shrinkage resin composite types, *J Oral Rehabil* **37**, 2010, 364–376.

[11]

G.L. Adabo, C.A. dos Santos Cruz, R.G. Fonseca and L.G. Vaz, The volumetric fraction of inorganic particles and the flexural strength of composites for posterior teeth, *J Dent* **31**, 2003, 353–359.

[12]

S. Beun, C. Bailly, A. Dabin, J. Vreven, J. Devaux and G. Leloup, Rheological properties of experimental Bis-GMA/TEGDMA flowable resin composites with various macrofiller/microfiller ratio, *Dent Mater* **25**, 2009, 198–205.

[13]

J.G. Leprince, M. Hadis, A.C. Shortall, J.L. Ferracane, J. Devaux, G. Leloup, et al., W.M.PalinPhotoinitiator type and applicability of exposure reciprocity law in filled and unfilled photoactive resins, *Dent Mater* 27, 2011, 157–164.

[14]

J.W. Stansbury and S.H. Dickens, Network formation and compositional drift during photo-initiated copolymerization of dimethacrylate monomers, *Polymer* 42, 2001, 6363–6369.

[15]

K.S. Anseth, L.M. Kline, T.A. Walker, K.J. Anderson and C.N. Bowman, Reaction Kinetics and Volume Relaxation during Polymerizations of Multiethylene Glycol Dkinetics and volume relaxation during polymerizations of multiethylene glycol dimethacrylates, *Macromolecules* 28, 1995, 2491–2499.

[16]

L. Musanje and B.W. Darvell, Curing-light attenuation in filled-resin restorative materials, *Dent Mater* 22, 2006, 804–817.

[17]

M. Wen, L.E. Scriven and A.V. McCormick, Kinetic Gelation Modeling: Kinetics of Cross-Linking Pgelation modeling: kinetics of cross-linking polymerization, *Macromolecules* 36, 2003, 4151–4159.

[18]

M.G. Neumann, C.C. Schmitt, G.C. Ferreira and I.C. Corrêa, The initiating radical yields and the efficiency of polymerization for various dental photoinitiators excited by different light curing units, *Dent Mater* 22, 2006, 576–584.

[19]

C. Decker, K. Zahouily, D. Decker, T. Nguyen and T. Viet, Performance analysis of acylphosphine oxides in photoinitiated polymerization, *Polymer* 42, 2001, 7551–7560.

[20]

K. Ikemura and T. Endo, A review of the development of radical photopolymerization initiators used for designing light-curing dental adhesives and resin composites, *Dental Materials Journal. Mater J* 29, 2010, 481–501.

[21]

L.D. Randolph, W.M. Palin, D.C. Watts, M. Genet, J. Devaux, G. Leloup, et al., J.G.LeprinceThe effect of ultra-fast photopolymerisation of experimental composites on shrinkage stress, network formation and pulpal temperature rise, *Dent Mater* 30, 2014, 1280–1289.

[22]

W.M. Palin, M.A. Hadis, J.G. Leprince, G. Leloup, L. Boland, G.J.P. Fleming, et al., G.KrastlD.C.WattsReduced polymerization stress of MAPO-containing resin composites with increased curing speed, degree of conversion and mechanical properties, *Dent Mater* 30, 2014, 507–516.

[23]

L.D. Randolph, W.M. Palin, S. Bebelman, J. Devaux, B. Gallez, G. Leloup, et al., J.G.LeprinceUltra-fast light-curing resin composite with increased conversion and reduced monomer elution, *Dent Mater* 30, 2014, 594–604.

[24]

J.W. Stansbury and S.H. Dickens, Determination of double bond conversion in dental resins by near infrared spectroscopy, *Dental Materials. Mater* 17, 2001, 71–79.

[25]

J. Steinhaus, B. Hausnerova, T. Haenel, M. Grossgarten and B. Moginger, Curing kinetics of visible light curing dental resin composites investigated by dielectric analysis (DEA), *Dent Mater* 30, 2014, 372–380.

[26]

J. Leprince, G. Lamblin, D. Truffier-Boutry, S. Demoustier-Champagne, J. Devaux, M. Mestdagh, et al., G.LeloupKinetic study of free radicals trapped in dental resins stored in different environments, *Acta Biomater* 5, 2009, 2518–2524.

[27]

R. Hardis, J.L.P. Jessop, F.E. Peters and M.R. Kessler, Cure kinetics characterization and monitoring of an epoxy resin using DSC, Raman spectroscopy, and DEA, *Composites Part A: Applied Science and Manufacturing. A: Appl Sci Manuf* 49, 2013, 100–108.

[28]

P.K. Shah and J.W. Stansbury, Role of filler and functional group conversion in the evolution of properties in polymeric dental restoratives, *Dent Mater* **30**, 2014, 586–593.

[29]

A.C. Shortall, W.M. Palin and P. Burtscher, Refractive index mismatch and monomer reactivity influence composite curing depth, *J Dent Res* **87**, 2008, 84–88.

[30]

M.A. Hadis, P.H. Tomlins, A.C. Shortall and W.M. Palin, Dynamic monitoring of refractive index change through photoactive resins, *Dent Mater* **26**, 2010, 1106–1112.

[31]

M.A. Hadis, A.C. Shortall and W.M. Palin, Specimen aspect ratio and light transmission in photoactive dental resins, *Dent Mater* **28**, 2012, 1154–1161.

[32]

W.D. Cook, Photopolymerization kinetics of oligo(ethylene oxide) and oligo(methylene) oxide dimethacrylates, *Polym Sci A: Polym Chem* **31**, 1993, 1053–1067.

[33]

J. Steinhaus, B. Moeginger, M. Grossgarten, M. Rosentritt and B. Hausnerova, Dielectric analysis of depth dependent curing behavior of dental resin composites, *Dent Mater* **30**, 2014, 679–687.

[34]

A. Schattenberg, D. Lichtenberg, E. Stender, B. Willershausen and C.P. Ernst, Minimal exposure time of different LED-curing devices, *Dent Mater* **24**, 2008, 1043–1049.

[35]

A.C. Shortall, C.J. Felix and D.C. Watts, Robust spectrometer-based methods for characterizing radiant exitance of dental LED light curing units, *Dent Mater* **31**, 2015, 339–350.

[36]

L.G. Lovelh, S.M. Newman and C.N. Bowman, The effects of light intensity, temperature, and comonomer composition on the polymerization behavior of dimethacrylate dental resins, *J Dent Res* **78**, 1999, 1469–1476.

[37]

L.G. Lovell, H. Lu, J.E. Elliott, J.W. Stansbury and C.N. Bowman, The effect of cure rate on the mechanical properties of dental resins, *Dent Mater* **17**, 2001, 504–511.

[38]

D.A. Abu-elenain, S.H. Lewis and J.W. Stansbury, Property evolution during vitrification of dimethacrylate photopolymer networks, *Dent Mater* **29**, 2013, 1173–1181.

[39]

V. Mucci, G. Arenas, R. Duchowicz, W.D. Cook and C. Vallo, Influence of thermal expansion on shrinkage during photopolymerization of dental resins based on bis-GMA/TEGDMA, *Dent Mater* **25**, 2009, 103–114.

[40]

M.G. Neumann, W.G. Miranda, Jr., C.C. Schmitt, F.A. Rueggeberg and I.C. Correa, Molar extinction coefficients and the photon absorption efficiency of dental photoinitiators and light curing units, *J Dent* **33**, 2005, 525–532.

[41]

K. Ikemura, K. Ichizawa, Y. Jogetsu and T. Endo, Synthesis of a novel camphorquinone derivative having acylphosphine oxide group, characterization by UV-VIS spectroscopy and evaluation of photopolymerization performance, *Dent Mater J* **29**, 2010, 122–131.

[42]

E. Andrzejewska, Photopolymerization kinetics of multifunctional monomers, *Polym Sci* **26**, 2001, 605–665.

[43]

K.S. Anseth and C.N. Bowman, Kinetic gelation model predictions of crosslinked polymer network microstructure, *Chem Eng Sci* **49**, 1994, 2207–2217.

[54]

J. Durner, W. Spahl, J. Zaspel, H. Schweikl, R. Hickel and F.-X. Reichl, Eluted substances from unpolymerized and polymerized dental restorative materials and their Nernst partition coefficient, *Mater* **26**, 2010, 91–99.

[65]

I.D. Sideridou and M.M. Karabela, Sorption of water, ethanol or ethanol/water solutions by light-cured dental dimethacrylate resins, *Mater* **27**, 2011, 1003–1010.

[76]

K.L. Van Landuyt, T. Nawrot, B. Geebelen, J. De Munck, J. Snauwaert, K. Yoshihara, et al., How much do resin-based dental materials release? A meta-analytical approach, *Dent Mater* **27**, 2011, 723–747.
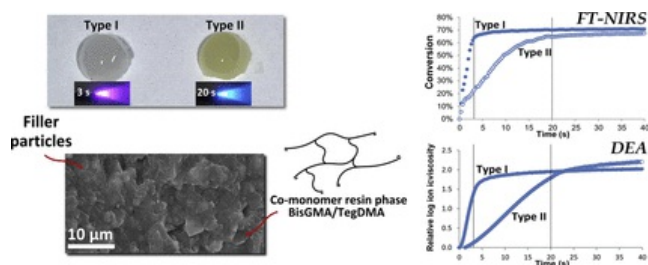
[87]

K.S. Chan, Y.D. Lee, D.P. Nicolella, B.R. Furman, S. Wellinghoff and H.R. Rawls, Improving fracture toughness of dental nanocomposites by interface engineering and micromechanics, *Eng Fract Mech* **74**, 2007, 1857–1871.

Appendix A. Supplementary data

The following are the supplementary data to this article:

Multimedia Component 1

Graphical abstract

Highlights

- MAPO and CQ-based filled resin composites were prepared using varying BisGMA/TegDMA formulations and photopolymerized for 3 or 20 s at 1000 mW/cm^2, respectively.

- Kinetics of polymerization were monitored using both FT-NIRS and DEA, providing complementary information and post-cure properties (monomer elution, trapped radical concentration and flexural modulus and strength) were also determined.

- Polymerization kinetics were faster with MAPO-composites, leading to equal or higher conversion than with CQ-composites, for all formulations.

- Initial ionic viscosity increased with BisGMA content and was associated with decreasing conversion, although to a lesser extent with MAPO-composites.

- 40 mol% BisGMA was required to reach a combined optimum in terms of conversion, monomer elution and mechanical properties, related to a balance between free and filler-bound monomer mobility. On the contrary, in CQ-composites, the highest properties were noted with 20 mol% BisGMA and only decreased with more viscous mixtures, highlighting a reduced efficiency compared to MAPO.

Queries and Answers

Query: Please confirm that given names and surnames have been identified correctly.

Answer: Yes

Query: Please check the telephone number of the corresponding author that has been added here, and correct if necessary.

Answer: The telephone number that should be used is: +32 27647345

Query: Highlights should consist of 3–5 bullet points and 85 characters per bullet point, including spaces. There are _ bullet points provided. Please edit the highlights to meet the requirement.

Answer: The length of the text was reduced to meet the requirements, except for item 2 which cannot be further amended: * MAPO and CQ-based filled resin composites were mixed using four BisGMA/TegDMA ratios. * Polymerization was monitored using both FT-NIRS and DEA and post-cure properties were also determined. * Initial ionic viscosity increased with BisGMA content, impacting final conversion. * Specific BisGMA contents were shown to be optimal (40 mol% - MAPO or ≤ 20 mol% - CQ). * Free and filler-bound monomer mobility and reactivity likely varied with the initiator.

Query: "Your article is registered as a regular item and is being processed for inclusion in a regular issue of the journal. If this is NOT correct and your article belongs to a Special Issue/Collection please contact m.renaud@elsevier.com immediately prior to returning your corrections.".

Answer: The article is a regular item.

Query: Please note that Refs. [9,31] were identical, and Ref. [31] has been deleted. The subsequent references have been renumbered.

Answer: Thank you for the modification.